Mathematical Biosciences and Engineering

MBE, 16(5): 5947–5971
DOI: 10.3934/mbe.2019298
Received: 21 March 2019
Accepted: 21 May 2019
Published: 27 June 2019

http://www.aimspress.com/journal/MBE

Research article

Integrative analysis reveals key mRNAs and lncRNAs in monocytes of osteoporotic patients

Li Li [1], Xueqing Wang [1], Xiaoting Liu [1], Rui Guo [2] and Ruidong Zhang [1,*]

[1] College of Life Sciences, Inner Mongolia Normal University, Hohhot, Inner Mongolia 010022, China
[2] Hefei Laboratory Center, Ping An Healthcare Investment Management Co, Ltd

*** Correspondence:** Email: zrd@imnu.edu.cn; Tel: +86-15848105596.

Abstract: Osteoporosis is the most common bone metabolic disease. Abnormal osteoclast formation and resorption play a fundamental role in osteoporosis pathogenesis. Recent researches have greatly broaden our understanding of molecular mechanisms of osteoporosis. However, the molecular mechanisms of key mRNAs and lncRNAs, and their interactions leading to osteoporosis are still not entirely clear. The purpose of this work is to study the key mRNAs and lncRNAs, and their interactions involved in bone mineral homeostasis and osteoclastogenesis. Systematic analyses such as differential expression analysis, GO and KEGG analysis, and PPI network construction revealed that up-regulated mRNAs were significantly enriched in inflammation-related pathways. Moreover, we observed that the down-regulated proteins, including JDP2, HADC4, HDAC5, CDYL2, ACADVL, ACSL1 and BRD4, were key components in the down-regulated PPI network, indicating that the downregulation of histone deacetylases and cofactors, such as, HDAC4, HDAC5 and JDP2 may be critical regulators in osteoclastogenesis. In addition, we also highlighted one lncRNA, RP11-498C9.17, was highly correlated with epigenetic regulators, such as HDAC4, MORF4L1, HMGA1 and DND1, indicating that the lncRNA RP11-498C9.17 may also be an epigenetic regulator. In conclusion, our integrative analysis reveals key mRNAs and lncRNAs, involved in bone mineral homeostasis and osteoclastogenesis, which not only broaden our insights into lncRNAs in bone mineral homeostasis and osteoclastogenesis, but also improve our understanding of molecular mechanism.

Keywords: Osteoporosis; osteoclastogenesis; key mRNAs and lncRNAs; molecular mechanism

1. Introduction

Osteoporosis (OP) is the most common bone disease characterized by a loss of bone mass and quality that results in fragility fractures. Osteoporosis is responsible for over 8.9 million fractures each year worldwide, with most cases occurring in postmenopausal women [1]. The most frequent osteoporotic fractures are fractures of the hip, wrist and spine, although most fractures in the elderly are probably at least partly related to osteoporosis. To prevent the osteoporosis, clinical risk factors [2–7], including age, female gender, rheumatoid arthritis, previous fragility fracture, genetic predisposition, smoking, >14 units of alcohol per week, early-onset menopause (<45 years of age) and low BMI (<19 kg per m^2), should be evaluated. To diagnose the osteoporosis, bone mineral density (BMD) measurement is widely used in clinical medicine as an indirect indicator of osteoporosis and fracture risk [8]. Specifically, the BMD measurement can category the subjects into four statuses, including normal, osteopenia, osteoporosis and severe osteoporosis.

Bone remodeling is accomplished by two specialized cells: bone-resorbing osteoclasts and bone-forming osteoblasts [9]. Osteoclasts can break down bone, while osteoblasts create new bone. Osteoclasts and osteoblasts can coordinate well for most of the human life [10]. In a pathological state of osteoporosis, this coordination can break down, and the osteoclasts begin to remove more bone than the osteoblasts can create [11]. To understand the molecular mechanism of osteoporosis, several studies introduced molecules, including SNP [12–15], DNA methylation [16], RNA [17] and microRNA [18], to investigate the genetic, epigenetic and transcriptomic regulators involved in osteoclastogenesis or osteoblastogenesis.

Osteoclastogenesis has been reported to cause osteoporosis by previous studies [19–21], however, the critical functional modules and signaling pathways still need to be explicitly characterized, which is useful for the discovery of the therapeutic targets in osteoclasts for the treatment of skeletal diseases. In this study, we collected gene expression datasets of peripheral blood monocytes (PBMs) from low or high BMD subjects. Notably, PBMs, which are osteoclast progenitor cells and produce cytokines for osteoclastogenesis and bone resorption, could be used for osteoporosis study. Furthermore, network based analysis and overrepresentation enrichment analysis highlighted critical functional modules and signaling pathways, which improved our understanding of the molecular mechanism, and provided the potential drug targets for osteoporosis.

2. Materials and method

2.1. Gene expression data pre-processing

Gene expression datasets were obtained from the NCBI Gene Expression Omnibus (GEO) (http://www.ncbi.nlm.nih.gov/geo) with accession numbers, GSE56814 [22]. Prior to downstream analysis, we firstly mapped the array probes to the GENCODE gene annotation v19. We calculated the average expression values of genes matching multiple probes.

2.2. Differential expression analysis

The differential expression analysis was conducted in R programming language (https://www.r-project.org) with student-t test. The differentially expressed genes were identified at

the threshold *P*-value <0.05. The up- or down-regulation status was determined based on the fold change for each gene.

2.3. *Overrepresentation enrichment analysis (OEA)*

Overrepresentation enrichment analysis was also implemented at WEB-based Gene Set Analysis Toolkit (WebGestalt) [23]. The Gene Ontology biological processes and KEGG pathways were selected as the functional database.

2.4. Protein-protein interaction network mapping

The Search Tool for the Retrieval of Interacting Genes/ Proteins (STRING) [24] online software (https://string-db.org) was used to assess the interactions. The interactions of the proteins encoded by the differently expressed genes were searched using STRING online software, and the combined score of >0.4 was used as the cut-off criterion. The PPI network was visualized using Cytoscape software (http://www.cytoscape.org). The Cytoscape MCODE plug-in (version 3.4.0) was applied to search for clustered sub-networks of highly connected nodes from the PPI network. The resulting network was subjected to module analyses with the Plugin MCODE with the following default parameters: Degree cut-off $\geqslant$3.

2.5. Construction of co-expression network between differentially expressed mRNAs and lncRNAs

The Pearson correlation coefficient of DEG-lncRNA pairs was calculated according to their expression values. The co-expressed DEG-lncRNA pairs with an absolute value of the Pearson correlation coefficient of $\geqslant$0.8 were selected and the co-expression network was visualized by using Cytoscape software.

3. Results

3.1. Identification of long non-coding RNAs by microarray probe reannotation

To identify the probes on the array corresponding to long non-coding RNA (lncRNA) sequences, we re-annotated all probes using GENCODE gene annotation with version 19. Finally, we identified a total of 830 long non-coding RNAs, with gene types such as processed transcript, antisense, long intergenic noncoding RNA (lincRNA) and pseudogene. We found that pseudogene accounted for the most of the identified lncRNAs (45%), followed by the long intergenic noncoding RNAs (29%, Figure 1A). In addition, the reannotation of the probes also mapped 17,051 probes to 17,743 protein-coding genes. We then compared the expression levels of lncRNAs with those of protein-coding genes, and found that expression levels were lower in lncRNAs than protein-coding genes (Figure 1B).

3.2. Differentially expressed mRNAs and lncRNAs

To uncover genes that may be responsible for osteoporosis, we compared the expression profiles

of low BMD subjects with that of high BMD subjects. We identified a total of 496 differentially expressed genes (DE-genes), including 120 up-regulated and 376 down-regulated genes in low BMD subjects (t-test, *P*-value <0.05, Supplementary Table 1). We observed that four zinc finger genes, ZNF528, ZNF79, ZNF223 and ZNF765, were included in the top-ten up-regulated genes, indicating that zinc finger genes may play key roles in osteoporosis. Notably, 24 lncRNAs were differentially expressed (DE) between samples with low and high BMD, which were presented in Supplementary Table 1. Visualization of the expression levels of DE-genes revealed that a fraction of normal controls (n = 15) exhibited similar expression patterns with the cases with low BMD (Figure 2). Furthermore, a higher proportion of postmenopausal normal controls were observed in the 15 samples than other normal controls (proportion test, P <0.05, 66.7% vs. 22.2%), suggesting that postmenopausal normal controls had a higher risk of osteoporosis.

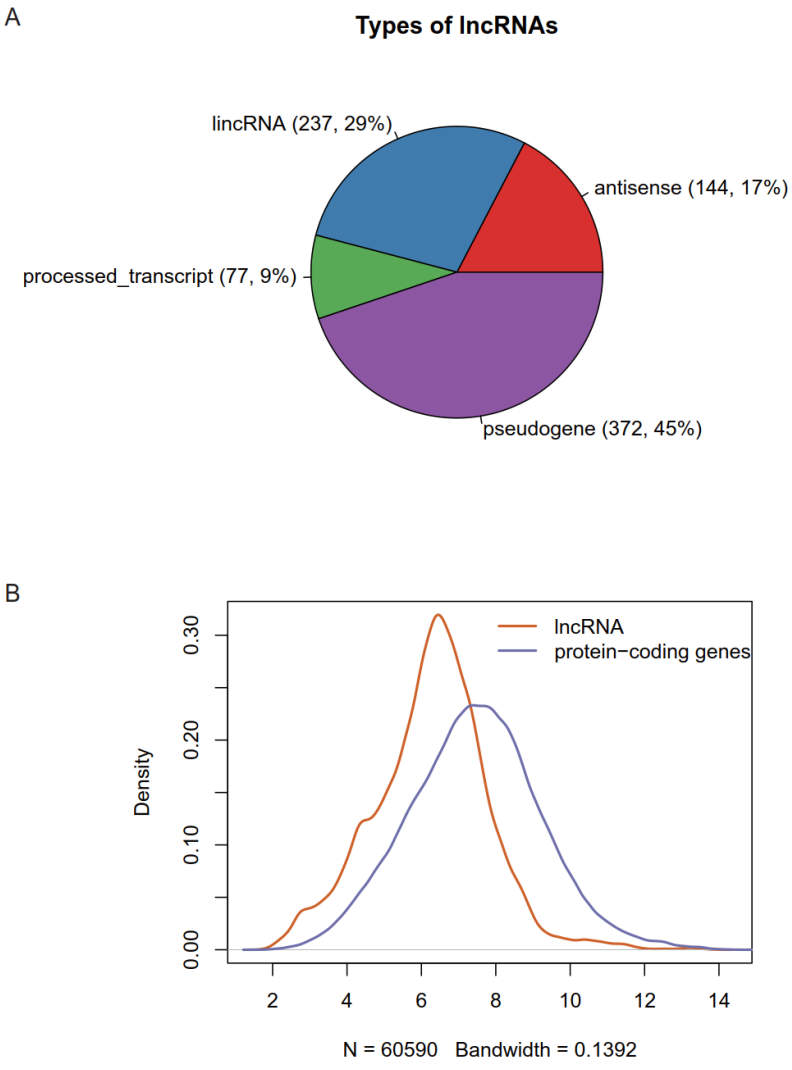

Figure 1. Identification of lncRNAs by reannotation of microarray probes. (A) The lncRNA categories, including pseudogene, processed transcript, antisense and lincRNA, counts and percentages are presented in pie chart with colors of purple, green, red and blue. (B) The expression distributions of lncRNAs and protein-coding mRNAs are represented by the red and purple lines.

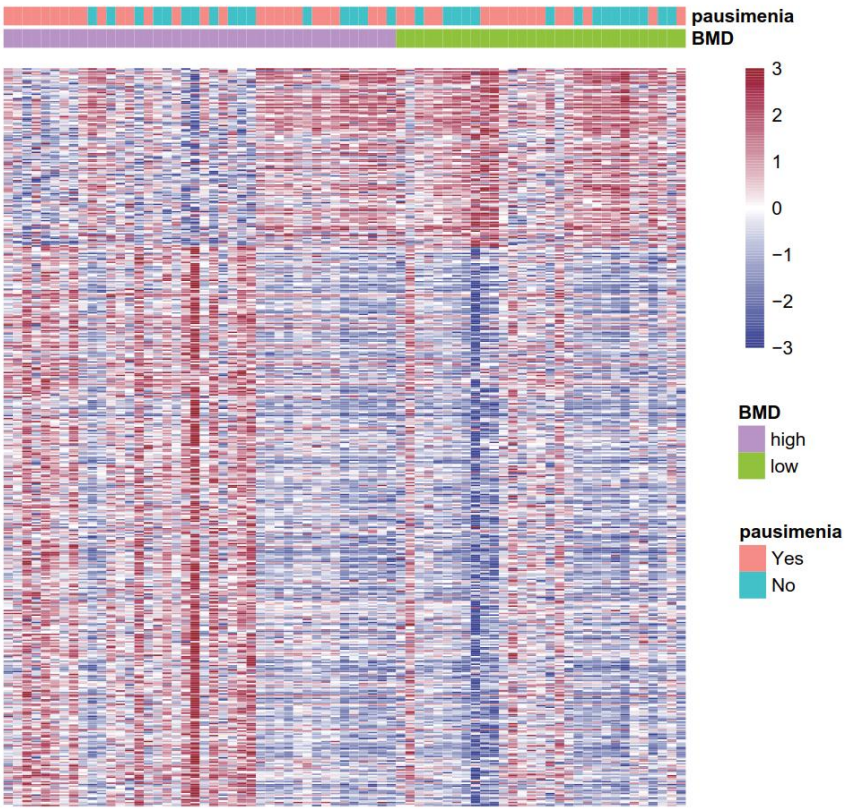

Figure 2. The gene expression levels of the differentially expressed genes across samples. The expression values are scaled by genes. The samples with high and low BMD are represented by the bands with pink and green, respectively. The premenopausal and postmenopausal samples are represented by the bands with green and red, respectively.

Table 1. A total of 496 differentially expressed genes (DE-genes), including 120 up-regulated and 376 down-regulated genes in low BMD subjects (t-test, *P*-value <0.05).

ID	gene_type	gene_symbol	status	p-value
ENSG00000001630.11	protein_coding	CYP51A1	Up	0.011965453
ENSG00000005075.11	protein_coding	POLR2J	Down	0.018005066
ENSG00000006282.15	protein_coding	SPATA20	Down	0.030683456
ENSG00000007376.3	protein_coding	RPUSD1	Down	0.046007757
ENSG00000007944.10	protein_coding	MYLIP	Up	0.012046727
ENSG00000008952.12	protein_coding	SEC62	Up	0.04688829
ENSG00000014164.6	protein_coding	ZC3H3	Down	0.035615575
ENSG00000020256.15	protein_coding	ZFP64	Up	0.035853374
ENSG00000025770.14	protein_coding	NCAPH2	Down	0.035381718
ENSG00000028277.16	protein_coding	POU2F2	Down	0.025284331
ENSG00000029153.10	protein_coding	ARNTL2	Down	0.010597798
ENSG00000032444.11	protein_coding	PNPLA6	Down	0.015278704
ENSG00000034533.7	protein_coding	ASTE1	Up	0.033013833
ENSG00000039123.11	protein_coding	SKIV2L2	Down	0.048932372

Continued on next page

ID	gene_type	gene_symbol	status	p-value
ENSG00000047056.10	protein_coding	WDR37	Down	0.034858116
ENSG00000050344.8	protein_coding	NFE2L3	Down	0.033023849
ENSG00000051523.6	protein_coding	CYBA	Down	0.007486695
ENSG00000052723.7	protein_coding	SIKE1	Up	0.045307581
ENSG00000052749.9	protein_coding	RRP12	Down	0.026396768
ENSG00000054803.3	protein_coding	CBLN4	Down	0.045582496
ENSG00000054967.8	protein_coding	RELT	Down	0.02019792
ENSG00000062598.13	protein_coding	ELMO2	Down	0.025904437
ENSG00000064932.11	protein_coding	SBNO2	Down	0.033420705
ENSG00000068024.12	protein_coding	HDAC4	Down	0.048895859
ENSG00000068120.10	protein_coding	COASY	Down	0.009649617
ENSG00000069764.5	protein_coding	PLA2G10	Down	0.003199821
ENSG00000070404.5	protein_coding	FSTL3	Down	0.038524776
ENSG00000072778.15	protein_coding	ACADVL	Down	0.028472324
ENSG00000074842.3	protein_coding	C19orf10	Down	0.00105098
ENSG00000077150.13	protein_coding	NFKB2	Down	0.003922325
ENSG00000078804.8	protein_coding	TP53INP2	Down	0.005193897
ENSG00000079393.16	protein_coding	DUSP13	Down	0.024246462
ENSG00000079432.3	protein_coding	CIC	Down	0.019836428
ENSG00000081189.9	protein_coding	MEF2C	Up	0.047860138
ENSG00000083312.13	protein_coding	TNPO1	Up	0.047418317
ENSG00000083844.6	protein_coding	ZNF264	Up	0.010459153
ENSG00000087157.14	protein_coding	PGS1	Down	0.042327569
ENSG00000087237.6	protein_coding	CETP	Down	0.032983061
ENSG00000087263.12	protein_coding	OGFOD1	Up	0.043418236
ENSG00000087266.11	protein_coding	SH3BP2	Down	0.030356676
ENSG00000087903.8	protein_coding	RFX2	Down	0.020836355
ENSG00000088888.13	protein_coding	MAVS	Down	0.04764586
ENSG00000089123.11	protein_coding	TASP1	Up	0.028910399
ENSG00000089248.6	protein_coding	ERP29	Down	0.049446948
ENSG00000089351.10	protein_coding	GRAMD1A	Down	0.025055632
ENSG00000089639.6	protein_coding	GMIP	Down	0.014587545
ENSG00000090924.10	protein_coding	PLEKHG2	Down	0.028301873
ENSG00000092929.7	protein_coding	UNC13D	Down	0.013293567
ENSG00000096088.12	protein_coding	PGC	Down	0.042062111
ENSG00000099139.9	protein_coding	PCSK5	Up	0.027380288
ENSG00000099203.2	protein_coding	TMED1	Down	0.028235039
ENSG00000099795.2	protein_coding	NDUFB7	Down	0.040697141
ENSG00000099800.3	protein_coding	TIMM13	Down	0.007324296
ENSG00000099821.9	protein_coding	POLRMT	Down	0.045124992
ENSG00000099958.10	protein_coding	DERL3	Down	0.04060876
ENSG00000099991.12	protein_coding	CABIN1	Down	0.034876772

Continued on next page

ID	gene_type	gene_symbol	status	p-value
ENSG00000100028.7	protein_coding	SNRPD3	Down	0.044318218
ENSG00000100055.16	protein_coding	CYTH4	Down	0.018939808
ENSG00000100092.16	protein_coding	SH3BP1	Down	0.04634582
ENSG00000100242.11	protein_coding	SUN2	Down	0.010030177
ENSG00000100290.2	protein_coding	BIK	Down	0.007141866
ENSG00000100403.10	protein_coding	ZC3H7B	Down	0.0410179
ENSG00000100429.13	protein_coding	HDAC10	Down	0.033877634
ENSG00000100532.7	protein_coding	CGRRF1	Up	0.013688977
ENSG00000100802.10	protein_coding	C14orf93	Down	0.033127459
ENSG00000100906.6	protein_coding	NFKBIA	Down	0.005259074
ENSG00000101220.13	protein_coding	C20orf27	Down	0.034454114
ENSG00000101473.12	protein_coding	ACOT8	Down	0.016141884
ENSG00000101624.6	protein_coding	CEP76	Up	0.013187998
ENSG00000101665.4	protein_coding	SMAD7	Down	0.017676506
ENSG00000101997.8	protein_coding	CCDC22	Down	0.039248809
ENSG00000102078.11	protein_coding	SLC25A14	Down	0.039031376
ENSG00000102786.10	protein_coding	INTS6	Up	0.044913283
ENSG00000102981.5	protein_coding	PARD6A	Down	0.041910914
ENSG00000103024.3	protein_coding	NME3	Down	0.027773943
ENSG00000103047.3	protein_coding	TANGO6	Down	0.049704948
ENSG00000103227.14	protein_coding	LMF1	Down	0.022119939
ENSG00000103426.8	protein_coding	CORO7-PAM16	Down	0.014976017
ENSG00000103449.7	protein_coding	SALL1	Down	0.041904944
ENSG00000103653.12	protein_coding	CSK	Down	0.010534323
ENSG00000104856.9	protein_coding	RELB	Down	0.015505238
ENSG00000104973.10	protein_coding	MED25	Down	0.041089276
ENSG00000105063.14	protein_coding	PPP6R1	Down	0.022586612
ENSG00000105135.11	protein_coding	ILVBL	Down	0.034386207
ENSG00000105497.3	protein_coding	ZNF175	Up	0.013075356
ENSG00000105643.5	protein_coding	ARRDC2	Down	0.039560218
ENSG00000105656.8	protein_coding	ELL	Down	0.035373441
ENSG00000106268.11	protein_coding	NUDT1	Down	0.03304039
ENSG00000107362.9	protein_coding	ABHD17B	Up	0.02410498
ENSG00000107443.11	protein_coding	CCNJ	Down	0.029817026
ENSG00000107984.5	protein_coding	DKK1	Down	0.049671011
ENSG00000108179.9	protein_coding	PPIF	Down	0.044960461
ENSG00000108518.7	protein_coding	PFN1	Down	0.045797043
ENSG00000108840.11	protein_coding	HDAC5	Down	0.01595402
ENSG00000108950.7	protein_coding	FAM20A	Down	0.012800605
ENSG00000109103.7	protein_coding	UNC119	Down	0.03809287
ENSG00000109736.10	protein_coding	MFSD10	Down	0.043758832
ENSG00000109917.6	protein_coding	ZNF259	Down	0.042419417

Continued on next page

ID	gene_type	gene_symbol	status	p-value
ENSG00000109944.6	protein_coding	C11orf63	Down	0.036421384
ENSG00000110063.4	protein_coding	DCPS	Down	0.044521345
ENSG00000110080.14	protein_coding	ST3GAL4	Down	0.009630116
ENSG00000110090.8	protein_coding	CPT1A	Down	0.040715917
ENSG00000110619.12	protein_coding	CARS	Down	0.040080075
ENSG00000110931.14	protein_coding	CAMKK2	Down	0.041840274
ENSG00000112149.5	protein_coding	CD83	Down	0.021210986
ENSG00000112276.9	protein_coding	BVES	Up	0.013370759
ENSG00000112312.5	protein_coding	GMNN	Down	0.047237299
ENSG00000114650.14	protein_coding	SCAP	Down	0.032838904
ENSG00000115073.6	protein_coding	ACTR1B	Down	0.003540043
ENSG00000116017.6	protein_coding	ARID3A	Down	0.038762022
ENSG00000116670.10	protein_coding	MAD2L2	Down	0.043537769
ENSG00000116852.10	protein_coding	KIF21B	Down	0.049989022
ENSG00000116871.11	protein_coding	MAP7D1	Down	0.03998345
ENSG00000116985.6	protein_coding	BMP8B	Down	0.028382633
ENSG00000117600.8	protein_coding	LPPR4	Down	0.046876942
ENSG00000118432.11	protein_coding	CNR1	Down	0.017637126
ENSG00000118600.7	protein_coding	TMEM5	Down	0.014944131
ENSG00000119013.4	protein_coding	NDUFB3	Down	0.040614225
ENSG00000119121.17	protein_coding	TRPM6	Down	0.048825853
ENSG00000119669.3	protein_coding	IRF2BPL	Down	0.005359191
ENSG00000120217.9	protein_coding	CD274	Down	0.043686299
ENSG00000120699.8	protein_coding	EXOSC8	Up	0.032500661
ENSG00000122203.10	protein_coding	KIAA1191	Up	0.048031425
ENSG00000122490.14	protein_coding	PQLC1	Down	0.015129367
ENSG00000122824.6	protein_coding	NUDT10	Down	0.033200739
ENSG00000123094.11	protein_coding	RASSF8	Down	0.029465179
ENSG00000123358.15	protein_coding	NR4A1	Down	0.01086372
ENSG00000123576.5	protein_coding	ESX1	Down	0.030485823
ENSG00000123689.5	protein_coding	G0S2	Down	0.009066817
ENSG00000123989.9	protein_coding	CHPF	Down	0.040386914
ENSG00000125657.3	protein_coding	TNFSF9	Down	0.049043875
ENSG00000125755.14	protein_coding	SYMPK	Down	0.049805392
ENSG00000125817.7	protein_coding	CENPB	Down	0.042137733
ENSG00000125945.10	protein_coding	ZNF436	Up	0.047416168
ENSG00000125968.7	protein_coding	ID1	Down	0.04512393
ENSG00000127054.14	protein_coding	CPSF3L	Down	0.04296422
ENSG00000127124.9	protein_coding	HIVEP3	Down	0.000294073
ENSG00000127483.13	protein_coding	HP1BP3	Up	0.047813073
ENSG00000127540.7	protein_coding	UQCR11	Down	0.030739395
ENSG00000127588.4	protein_coding	GNG13	Down	0.039828869

Continued on next page

ID	gene_type	gene_symbol	status	p-value
ENSG00000128059.4	protein_coding	PPAT	Up	0.006604019
ENSG00000128228.4	protein_coding	SDF2L1	Down	0.003273018
ENSG00000128271.15	protein_coding	ADORA2A	Down	0.041530393
ENSG00000128309.12	protein_coding	MPST	Down	0.037538756
ENSG00000128694.7	protein_coding	OSGEPL1	Up	0.036634744
ENSG00000129562.6	protein_coding	DAD1	Up	0.039222956
ENSG00000129667.8	protein_coding	RHBDF2	Down	0.030796176
ENSG00000129744.2	protein_coding	ART1	Down	0.001540155
ENSG00000129968.11	protein_coding	ABHD17A	Down	0.043478487
ENSG00000129993.10	protein_coding	CBFA2T3	Down	0.031277467
ENSG00000130522.4	protein_coding	JUND	Down	0.022542768
ENSG00000130766.4	protein_coding	SESN2	Down	0.013640369
ENSG00000130935.5	protein_coding	NOL11	Up	0.044393023
ENSG00000131142.9	protein_coding	CCL25	Down	0.038185878
ENSG00000131171.8	protein_coding	SH3BGRL	Up	0.022819598
ENSG00000131653.8	protein_coding	TRAF7	Down	0.036084131
ENSG00000131849.10	protein_coding	ZNF132	Down	0.028132404
ENSG00000132275.6	protein_coding	RRP8	Down	0.010570164
ENSG00000132507.13	protein_coding	EIF5A	Down	0.024112694
ENSG00000133606.6	protein_coding	MKRN1	Up	0.041317442
ENSG00000133805.11	protein_coding	AMPD3	Down	0.046431783
ENSG00000134107.4	protein_coding	BHLHE40	Down	0.038744934
ENSG00000135047.10	protein_coding	CTSL	Down	0.0255056
ENSG00000135390.13	protein_coding	ATP5G2	Down	0.02929579
ENSG00000136048.9	protein_coding	DRAM1	Down	0.02091681
ENSG00000136122.11	protein_coding	BORA	Up	0.036657962
ENSG00000136738.10	protein_coding	STAM	Up	0.0389495
ENSG00000136840.14	protein_coding	ST6GALNAC4	Down	0.016088565
ENSG00000136877.10	protein_coding	FPGS	Down	0.023271049
ENSG00000137124.6	protein_coding	ALDH1B1	Up	0.03438067
ENSG00000137193.9	protein_coding	PIM1	Down	0.009876567
ENSG00000137218.6	protein_coding	FRS3	Down	0.042976435
ENSG00000137309.15	protein_coding	HMGA1	Down	0.021493168
ENSG00000137312.10	protein_coding	FLOT1	Down	0.039597455
ENSG00000137409.14	protein_coding	MTCH1	Down	0.040766375
ENSG00000138382.9	protein_coding	METTL5	Up	0.038252044
ENSG00000139053.2	protein_coding	PDE6H	Down	0.0207692
ENSG00000139610.1	protein_coding	CELA1	Up	0.038317749
ENSG00000139668.7	protein_coding	WDFY2	Down	0.019753557
ENSG00000140044.8	protein_coding	JDP2	Down	0.036877537
ENSG00000140553.12	protein_coding	UNC45A	Down	0.042323486
ENSG00000140612.9	protein_coding	SEC11A	Down	0.017070625

Continued on next page

ID	gene_type	gene_symbol	status	p-value
ENSG00000140848.12	protein_coding	CPNE2	Down	0.035194471
ENSG00000140941.8	protein_coding	MAP1LC3B	Up	0.010046471
ENSG00000141012.8	protein_coding	GALNS	Down	0.019933327
ENSG00000141034.5	protein_coding	GID4	Up	0.036023887
ENSG00000141198.9	protein_coding	TOM1L1	Down	0.043796522
ENSG00000141252.15	protein_coding	VPS53	Down	0.020821593
ENSG00000141505.7	protein_coding	ASGR1	Down	0.049034425
ENSG00000141646.9	protein_coding	SMAD4	Up	0.041545876
ENSG00000141867.13	protein_coding	BRD4	Down	0.040247622
ENSG00000142408.2	protein_coding	CACNG8	Down	0.035337949
ENSG00000142538.1	protein_coding	PTH2	Down	0.028959056
ENSG00000143549.15	protein_coding	TPM3	Down	0.005503969
ENSG00000144120.8	protein_coding	TMEM177	Up	0.022405325
ENSG00000144182.12	protein_coding	LIPT1	Up	0.008805655
ENSG00000144381.12	protein_coding	HSPD1	Down	0.048940793
ENSG00000144468.12	protein_coding	RHBDD1	Up	0.048354944
ENSG00000144655.10	protein_coding	CSRNP1	Down	0.03240296
ENSG00000144791.5	protein_coding	LIMD1	Down	0.04142983
ENSG00000144802.7	protein_coding	NFKBIZ	Down	0.015266617
ENSG00000145901.10	protein_coding	TNIP1	Down	0.031453499
ENSG00000146047.4	protein_coding	HIST1H2BA	Down	0.005162611
ENSG00000146232.10	protein_coding	NFKBIE	Down	0.020469032
ENSG00000146828.13	protein_coding	SLC12A9	Down	0.042442305
ENSG00000146833.11	protein_coding	TRIM4	Up	0.001031314
ENSG00000146856.10	protein_coding	AGBL3	Down	0.044096515
ENSG00000147419.12	protein_coding	CCDC25	Up	0.027233589
ENSG00000148187.13	protein_coding	MRRF	Up	0.01456252
ENSG00000148335.10	protein_coding	NTMT1	Down	0.033476509
ENSG00000148602.5	protein_coding	LRIT1	Down	0.038378276
ENSG00000148737.11	protein_coding	TCF7L2	Down	0.03027628
ENSG00000148835.9	protein_coding	TAF5	Up	0.017608599
ENSG00000149115.9	protein_coding	TNKS1BP1	Down	0.031874191
ENSG00000149503.8	protein_coding	INCENP	Down	0.039618744
ENSG00000149792.4	protein_coding	MRPL49	Down	0.014313227
ENSG00000149823.3	protein_coding	VPS51	Down	0.034228234
ENSG00000149932.12	protein_coding	TMEM219	Down	0.042059762
ENSG00000149968.7	protein_coding	MMP3	Down	0.007039867
ENSG00000151093.3	protein_coding	OXSM	Up	0.032113374
ENSG00000151490.9	protein_coding	PTPRO	Down	0.0169847
ENSG00000151631.7	pseudogene	AKR1C6P	Down	0.004333285
ENSG00000151651.11	protein_coding	ADAM8	Down	0.034809828
ENSG00000151726.9	protein_coding	ACSL1	Down	0.040278414

Continued on next page

ID	gene_type	gene_symbol	status	p-value
ENSG00000152207.3	protein_coding	CYSLTR2	Up	0.031075114
ENSG00000152382.5	protein_coding	TADA1	Down	0.034551617
ENSG00000153140.4	protein_coding	CETN3	Up	0.028301839
ENSG00000153207.10	protein_coding	AHCTF1	Down	0.014567315
ENSG00000153266.8	protein_coding	FEZF2	Down	0.036977261
ENSG00000153487.11	protein_coding	ING1	Down	0.015188879
ENSG00000154370.9	protein_coding	TRIM11	Down	0.018777551
ENSG00000154447.10	protein_coding	SH3RF1	Down	0.009674391
ENSG00000154639.14	protein_coding	CXADR	Down	0.00685789
ENSG00000154781.11	protein_coding	CCDC174	Down	0.049642675
ENSG00000154839.5	protein_coding	SKA1	Down	0.046702852
ENSG00000154978.8	protein_coding	VOPP1	Down	0.030307149
ENSG00000155438.7	protein_coding	MKI67IP	Down	0.03414805
ENSG00000155918.3	protein_coding	RAET1L	Down	0.047085308
ENSG00000156172.5	protein_coding	C8orf37	Up	0.015241022
ENSG00000156508.13	protein_coding	EEF1A1	Down	0.029958858
ENSG00000157227.8	protein_coding	MMP14	Down	0.018623306
ENSG00000157326.14	protein_coding	DHRS4	Down	0.047099568
ENSG00000157456.3	protein_coding	CCNB2	Down	0.012184904
ENSG00000157637.8	protein_coding	SLC38A10	Down	0.026642558
ENSG00000158014.10	protein_coding	SLC30A2	Down	0.026315721
ENSG00000158483.11	protein_coding	FAM86C1	Down	0.00975309
ENSG00000158497.2	protein_coding	HMHB1	Down	0.040327646
ENSG00000158555.10	protein_coding	GDPD5	Down	0.034837228
ENSG00000159069.9	protein_coding	FBXW5	Down	0.01907369
ENSG00000159885.9	protein_coding	ZNF222	Up	0.01199585
ENSG00000160111.8	protein_coding	CPAMD8	Down	0.049299496
ENSG00000160179.14	protein_coding	ABCG1	Up	0.022299138
ENSG00000160180.14	protein_coding	TFF3	Down	0.042914253
ENSG00000160214.8	protein_coding	RRP1	Down	0.049738569
ENSG00000160796.12	protein_coding	NBEAL2	Down	0.035908182
ENSG00000160883.6	protein_coding	HK3	Down	0.044846812
ENSG00000160888.6	protein_coding	IER2	Down	0.027407148
ENSG00000161640.11	protein_coding	SIGLEC11	Down	0.042121328
ENSG00000161791.9	protein_coding	FMNL3	Down	0.011008036
ENSG00000162086.10	protein_coding	ZNF75A	Up	0.019226079
ENSG00000162302.8	protein_coding	RPS6KA4	Down	0.048212217
ENSG00000162377.4	protein_coding	SELRC1	Up	0.047979072
ENSG00000162413.12	protein_coding	KLHL21	Down	0.048454407
ENSG00000162522.6	protein_coding	KIAA1522	Down	0.016306649
ENSG00000162783.8	protein_coding	IER5	Down	0.021919966
ENSG00000162913.9	protein_coding	C1orf145	Down	0.018777551

Continued on next page

ID	gene_type	gene_symbol	status	p-value
ENSG00000162927.9	protein_coding	PUS10	Up	0.04033551
ENSG00000162931.7	protein_coding	TRIM17	Down	0.023650474
ENSG00000163162.4	protein_coding	RNF149	Down	0.025666014
ENSG00000163239.8	protein_coding	TDRD10	Down	0.043592404
ENSG00000163389.6	protein_coding	POGLUT1	Up	0.022081661
ENSG00000163947.7	protein_coding	ARHGEF3	Up	0.010264753
ENSG00000164105.3	protein_coding	SAP30	Up	0.046694723
ENSG00000164342.8	protein_coding	TLR3	Up	0.003277358
ENSG00000164402.9	protein_coding	8-Sep	Down	0.024177765
ENSG00000164411.6	protein_coding	GJB7	Down	0.026747052
ENSG00000165029.11	protein_coding	ABCA1	Up	0.010492577
ENSG00000165188.9	protein_coding	RNF183	Down	0.010089847
ENSG00000165406.11	protein_coding	8-Mar	Up	0.047180108
ENSG00000165512.4	protein_coding	ZNF22	Up	0.033208827
ENSG00000165782.6	protein_coding	TMEM55B	Down	0.022652362
ENSG00000165886.4	protein_coding	UBTD1	Down	0.014531961
ENSG00000165915.9	protein_coding	SLC39A13	Down	0.024410393
ENSG00000166265.7	protein_coding	CYYR1	Down	0.037657919
ENSG00000166363.4	protein_coding	OR10A5	Up	0.018183215
ENSG00000166446.10	protein_coding	CDYL2	Down	0.011853205
ENSG00000166451.9	protein_coding	CENPN	Up	0.040214671
ENSG00000166452.7	protein_coding	AKIP1	Up	0.048924644
ENSG00000166938.8	protein_coding	DIS3L	Up	0.036638539
ENSG00000166974.8	protein_coding	MAPRE2	Up	0.048488455
ENSG00000167110.12	protein_coding	GOLGA2	Down	0.023994018
ENSG00000167186.6	protein_coding	COQ7	Up	0.000296612
ENSG00000167333.8	protein_coding	TRIM68	Up	0.039246931
ENSG00000167394.8	protein_coding	ZNF668	Down	0.015855291
ENSG00000167414.4	protein_coding	GNG8	Down	0.0489265
ENSG00000167555.9	protein_coding	ZNF528	Up	0.002098542
ENSG00000167604.9	protein_coding	NFKBID	Down	0.04908962
ENSG00000167657.7	protein_coding	DAPK3	Down	0.045503987
ENSG00000168066.16	protein_coding	SF1	Down	0.047265519
ENSG00000168310.6	protein_coding	IRF2	Up	0.044253405
ENSG00000168594.11	protein_coding	ADAM29	Down	0.003444856
ENSG00000168803.10	protein_coding	ADAL	Up	0.021101681
ENSG00000168818.5	protein_coding	STX18	Up	0.022001045
ENSG00000168967.10	pseudogene	PMCHL1	Down	0.008435479
ENSG00000169105.6	protein_coding	CHST14	Down	0.024636798
ENSG00000169379.11	protein_coding	ARL13B	Up	0.010209654
ENSG00000169393.4	protein_coding	ELSPBP1	Down	0.014495593
ENSG00000169429.6	protein_coding	IL8	Down	0.028420528

Continued on next page

ID	gene_type	gene_symbol	status	p-value
ENSG00000170265.7	protein_coding	ZNF282	Down	0.042671468
ENSG00000170369.3	protein_coding	CST2	Down	0.041604924
ENSG00000170445.8	protein_coding	HARS	Down	0.029725289
ENSG00000170779.10	protein_coding	CDCA4	Down	0.028547735
ENSG00000170837.2	protein_coding	GPR27	Down	0.035077639
ENSG00000170891.6	protein_coding	CYTL1	Down	0.032834474
ENSG00000171130.13	protein_coding	ATP6V0E2	Down	0.039784296
ENSG00000171223.4	protein_coding	JUNB	Down	0.038177458
ENSG00000171357.5	protein_coding	LURAP1	Down	0.033100787
ENSG00000171467.11	protein_coding	ZNF318	Down	0.044327394
ENSG00000171530.9	protein_coding	TBCA	Down	0.009876223
ENSG00000171570.6	protein_coding	RAB4B-EGLN2	Down	0.010162577
ENSG00000171657.5	protein_coding	GPR82	Up	0.002688119
ENSG00000171766.11	protein_coding	GATM	Up	0.035375608
ENSG00000171827.6	protein_coding	ZNF570	Up	0.016772935
ENSG00000171861.6	protein_coding	RNMTL1	Down	0.041110394
ENSG00000171942.3	protein_coding	OR10H2	Down	0.01466908
ENSG00000172208.3	protein_coding	OR4X2	Up	0.038143037
ENSG00000172322.9	protein_coding	CLEC12A	Up	0.008850366
ENSG00000172375.8	protein_coding	C2CD2L	Down	0.012079432
ENSG00000172428.6	protein_coding	MYEOV2	Down	0.025783713
ENSG00000173020.6	protein_coding	ADRBK1	Down	0.043055525
ENSG00000173153.9	protein_coding	ESRRA	Down	0.008541886
ENSG00000173653.3	protein_coding	RCE1	Down	0.030649495
ENSG00000173715.11	protein_coding	C11orf80	Down	0.030649495
ENSG00000173812.6	protein_coding	EIF1	Down	0.0170157
ENSG00000173846.8	protein_coding	PLK3	Down	0.015509349
ENSG00000174600.9	protein_coding	CMKLR1	Up	0.044214317
ENSG00000174886.8	protein_coding	NDUFA11	Down	0.022192837
ENSG00000175130.6	protein_coding	MARCKSL1	Down	0.038863502
ENSG00000175728.2	protein_coding	C11orf44	Up	0.045296195
ENSG00000175874.5	protein_coding	CREG2	Down	0.01537001
ENSG00000176485.6	protein_coding	PLA2G16	Down	0.024862828
ENSG00000176563.5	protein_coding	CNTD1	Down	0.016145384
ENSG00000176619.6	protein_coding	LMNB2	Down	0.030268302
ENSG00000176624.9	protein_coding	MEX3C	Up	0.029845716
ENSG00000176714.9	protein_coding	CCDC121	Down	0.022706601
ENSG00000176749.4	protein_coding	CDK5R1	Down	0.04550598
ENSG00000176845.8	protein_coding	METRNL	Down	0.010677297
ENSG00000176894.5	protein_coding	PXMP2	Down	0.013611729
ENSG00000176974.13	protein_coding	SHMT1	Up	0.049830843
ENSG00000177051.5	protein_coding	FBXO46	Down	0.047542187

Continued on next page

ID	gene_type	gene_symbol	status	p-value
ENSG00000177169.5	protein_coding	ULK1	Down	0.016389135
ENSG00000177666.11	protein_coding	PNPLA2	Down	0.043015592
ENSG00000178229.7	protein_coding	ZNF543	Up	0.010459153
ENSG00000178951.4	protein_coding	ZBTB7A	Down	0.019056001
ENSG00000178980.10	protein_coding	SEPW1	Down	0.016556027
ENSG00000179029.10	protein_coding	TMEM107	Down	0.005945219
ENSG00000180008.8	protein_coding	SOCS4	Up	0.039599073
ENSG00000180332.5	protein_coding	KCTD4	Down	0.022125509
ENSG00000180346.2	protein_coding	TIGD2	Up	0.037693259
ENSG00000180539.4	protein_coding	C9orf139	Down	0.01622825
ENSG00000180725.4	pseudogene	AC015871.1	Down	0.042511409
ENSG00000181378.9	protein_coding	CCDC108	Down	0.038235948
ENSG00000181791.1	pseudogene	AC009041.1	Down	0.0167024
ENSG00000182118.5	protein_coding	FAM89A	Down	0.002426708
ENSG00000182333.10	protein_coding	LIPF	Down	0.018324226
ENSG00000182368.4	protein_coding	FAM27A	Down	0.03035551
ENSG00000182541.13	protein_coding	LIMK2	Down	0.041747303
ENSG00000182782.7	protein_coding	HCAR2	Down	0.046508935
ENSG00000182841.8	pseudogene	RRP7B	Down	0.04819365
ENSG00000183019.3	protein_coding	C19orf59	Down	0.031283921
ENSG00000183020.9	protein_coding	AP2A2	Down	0.000692239
ENSG00000183087.10	protein_coding	GAS6	Down	0.026705611
ENSG00000183648.5	protein_coding	NDUFB1	Down	0.00863385
ENSG00000183696.9	protein_coding	UPP1	Down	0.021571741
ENSG00000183709.7	protein_coding	IFNL2	Up	0.001410201
ENSG00000183723.8	protein_coding	CMTM4	Down	0.047938821
ENSG00000183779.5	protein_coding	ZNF703	Down	0.033061055
ENSG00000184110.10	protein_coding	EIF3C	Down	0.008205594
ENSG00000184517.7	protein_coding	ZFP1	Up	0.045781579
ENSG00000184619.3	protein_coding	KRBA2	Down	0.025225822
ENSG00000184897.4	protein_coding	H1FX	Down	0.014748614
ENSG00000184922.9	protein_coding	FMNL1	Down	0.01035533
ENSG00000184990.8	protein_coding	SIVA1	Down	0.039061925
ENSG00000185641.5	pseudogene	CTD-2287O16.1	Down	0.043078899
ENSG00000185787.10	protein_coding	MORF4L1	Down	0.047667026
ENSG00000185972.4	protein_coding	CCIN	Down	0.044995407
ENSG00000186106.7	protein_coding	ANKRD46	Up	0.042420836
ENSG00000186111.4	protein_coding	PIP5K1C	Down	0.042436011
ENSG00000186281.8	protein_coding	GPAT2	Down	0.049178673
ENSG00000186594.8	lincRNA	MIR22HG	Down	0.017511035
ENSG00000186635.10	protein_coding	ARAP1	Down	0.015438232
ENSG00000186795.1	protein_coding	KCNK18	Down	0.020856507

Continued on next page

ID	gene_type	gene_symbol	status	p-value
ENSG00000187630.10	protein_coding	DHRS4L2	Down	0.047099568
ENSG00000187688.10	protein_coding	TRPV2	Down	0.003137583
ENSG00000188379.5	protein_coding	IFNA2	Down	0.004976237
ENSG00000189042.9	protein_coding	ZNF567	Up	0.015774858
ENSG00000189114.6	protein_coding	BLOC1S3	Down	0.028793638
ENSG00000189332.4	protein_coding	RP11-113D6.10	Down	0.029127001
ENSG00000196152.6	protein_coding	ZNF79	Up	0.002879344
ENSG00000196331.5	protein_coding	HIST1H2BO	Down	0.025404112
ENSG00000196358.6	protein_coding	NTNG2	Down	0.042750195
ENSG00000196371.2	protein_coding	FUT4	Down	0.011093343
ENSG00000196415.5	protein_coding	PRTN3	Down	0.035149627
ENSG00000196417.8	protein_coding	ZNF765	Up	0.005727824
ENSG00000196652.7	protein_coding	ZKSCAN5	Up	0.016188909
ENSG00000196668.3	processed_transcript	LINC00173	Down	0.003213639
ENSG00000196693.10	protein_coding	ZNF33B	Up	0.010400288
ENSG00000196843.11	protein_coding	ARID5A	Down	0.023473729
ENSG00000196917.4	protein_coding	HCAR1	Down	0.023288331
ENSG00000196981.2	protein_coding	WDR5B	Up	0.010645113
ENSG00000197016.7	protein_coding	ZNF470	Up	0.021502777
ENSG00000197312.7	protein_coding	DDI2	Up	0.049559262
ENSG00000197321.10	protein_coding	SVIL	Down	0.029323831
ENSG00000197919.3	protein_coding	IFNA1	Down	0.011997429
ENSG00000198055.6	protein_coding	GRK6	Down	0.018617852
ENSG00000198081.6	protein_coding	ZBTB14	Up	0.03828373
ENSG00000198324.10	protein_coding	FAM109A	Down	0.015387399
ENSG00000198445.3	protein_coding	CCT8L2	Down	0.008263414
ENSG00000198464.9	protein_coding	ZNF480	Up	0.04695864
ENSG00000198471.1	protein_coding	RTP2	Up	0.026862674
ENSG00000198551.5	protein_coding	ZNF627	Up	0.007529781
ENSG00000198754.5	protein_coding	OXCT2	Down	0.028382633
ENSG00000198830.6	protein_coding	HMGN2	Down	0.034053765
ENSG00000198881.8	protein_coding	ASB12	Down	0.042963309
ENSG00000198900.5	protein_coding	TOP1	Up	0.036803174
ENSG00000198914.2	protein_coding	POU3F3	Down	0.040875916
ENSG00000198945.3	protein_coding	L3MBTL3	Up	0.040353636
ENSG00000198954.4	protein_coding	KIAA1279	Up	0.014789739
ENSG00000198967.3	protein_coding	OR10Z1	Down	0.02892736
ENSG00000203326.5	protein_coding	ZNF525	Up	0.019737784
ENSG00000203684.5	protein_coding	IBA57-AS1	Down	0.018777551
ENSG00000204807.1	protein_coding	FAM27E2	Down	0.03035551
ENSG00000204983.8	protein_coding	PRSS1	Down	0.022866585
ENSG00000205022.5	protein_coding	PABPN1L	Down	0.031277467

Continued on next page

ID	gene_type	gene_symbol	status	p-value
ENSG00000205409.3	protein_coding	OR52E6	Up	0.039983429
ENSG00000212916.3	protein_coding	MAP10	Down	0.04462334
ENSG00000213799.6	protein_coding	ZNF845	Up	0.019737784
ENSG00000213828.1	protein_coding	AC017028.1	Down	0.026268434
ENSG00000213888.2	protein_coding	AC005003.1	Down	0.030588957
ENSG00000214253.4	protein_coding	FIS1	Down	0.036530674
ENSG00000215612.5	protein_coding	HMX1	Down	0.030423062
ENSG00000215695.1	protein_coding	RSC1A1	Up	0.049559262
ENSG00000217930.3	protein_coding	PAM16	Down	0.014976017
ENSG00000220848.4	pseudogene	RPS18P9	Down	0.024449402
ENSG00000221837.4	protein_coding	KRTAP10-9	Down	0.028181439
ENSG00000221840.2	protein_coding	OR4A5	Down	0.013014151
ENSG00000221949.2	protein_coding	C12orf61	Down	0.031578862
ENSG00000221954.2	protein_coding	OR4C12	Down	0.010582213
ENSG00000224474.2	protein_coding	AL355490.1	Down	0.026396768
ENSG00000228300.9	protein_coding	C19orf24	Down	0.046090199
ENSG00000228336.1	pseudogene	OR9H1P	Down	0.031871552
ENSG00000230257.1	antisense	NFE4	Down	0.021397338
ENSG00000232973.7	antisense	CYP1B1-AS1	Up	0.031113526
ENSG00000233016.2	antisense	SNHG7	Down	0.048765474
ENSG00000236773.1	pseudogene	RP11-365O16.1	Up	0.015477893
ENSG00000237541.3	protein_coding	HLA-DQA2	Up	0.020285026
ENSG00000238184.1	processed_transcript	AC129929.5	Down	0.040824827
ENSG00000240720.3	protein_coding	LRRD1	Up	0.006393288
ENSG00000240970.1	pseudogene	RPL23AP64	Down	0.000986343
ENSG00000241360.1	protein_coding	PDXP	Down	0.04634582
ENSG00000244623.1	protein_coding	OR2AE1	Up	0.001031314
ENSG00000245680.5	protein_coding	ZNF585B	Up	0.029339876
ENSG00000247077.2	protein_coding	PGAM5	Down	0.03099048
ENSG00000251357.4	protein_coding	AP000350.10	Down	0.044557673
ENSG00000254521.2	protein_coding	SIGLEC12	Up	0.008757157
ENSG00000255769.3	pseudogene	RP11-152F13.3	Down	0.031901455
ENSG00000255804.1	protein_coding	OR6J1	Up	0.039222956
ENSG00000256235.1	protein_coding	SMIM3	Down	0.036368455
ENSG00000256294.3	protein_coding	ZNF225	Up	0.046416681
ENSG00000256453.1	protein_coding	DND1	Down	0.023504581
ENSG00000256632.3	protein_coding	RP13-672B3.2	Down	0.013611729
ENSG00000256683.2	protein_coding	ZNF350	Up	0.021879236
ENSG00000257341.1	protein_coding	CRIP1	Down	0.049720545
ENSG00000257702.3	antisense	LBX2-AS1	Down	0.035045107
ENSG00000258405.5	protein_coding	ZNF578	Down	0.021484975
ENSG00000258472.4	protein_coding	RP11-192H23.4	Down	0.047286987

Continued on next page

ID	gene_type	gene_symbol	status	p-value
ENSG00000259571.1	protein_coding	BLID	Down	0.02508268
ENSG00000261713.2	processed_transcript	SSTR5-AS1	Down	0.0167024
ENSG00000263002.3	protein_coding	ZNF234	Up	0.035012293
ENSG00000263620.1	protein_coding	RP11-599B13.6	Down	0.04868739
ENSG00000263809.1	protein_coding	RP11-849F2.7	Down	0.025225822
ENSG00000264735.1	lincRNA	RP11-498C9.17	Down	0.038254904
ENSG00000267022.1	protein_coding	ZNF223	Up	0.005281393
ENSG00000267059.2	protein_coding	UQCR11	Down	0.01521352
ENSG00000267360.2	protein_coding	CTC-454I21.3	Up	0.036745114
ENSG00000267545.1	protein_coding	AC005779.2	Down	0.028793638
ENSG00000267699.2	protein_coding	RP11-729L2.2	Up	0.041545876
ENSG00000268614.1	protein_coding	CTD-2207O23.10	Down	0.021055407
ENSG00000268797.1	protein_coding	CTC-490E21.12	Down	0.003100426
ENSG00000269220.1	lincRNA	LINC00528	Down	0.026695365
ENSG00000269636.1	protein_coding	AC010441.1	Down	0.036368455
ENSG00000269858.1	protein_coding	EGLN2	Down	0.003100426
ENSG00000271810.1	protein_coding	RP11-426L16.10	Down	0.02868524
ENSG00000271959.1	antisense	CTD-3064M3.7	Down	0.036335334
ENSG00000272906.1	lincRNA	RP11-533E19.7	Down	0.011437491
ENSG00000273006.1	lincRNA	RP11-314C9.2	Up	0.031113526

3.3. GO and KEGG enrichment analysis

Next, the differentially expressed mRNAs were subjected to GO and KEGG analyses (Figure 2). GO analysis indicated that the upregulated genes were mainly involved in regulating nucleobase metabolic process, regulation of organelle assembly, regulation of plasma lipoprotein particle levels, response to interferon-gamma, snRNA metabolic process, ncRNA transcription and ncRNA processing (Figure 3A). Furthermore, the downregulated genes were mainly enriched in categories associated with regulation of sequence-specific DNA binding transcription factor activity, neutral lipid metabolic process, cytokinesis, nucleoside triphosphate metabolic process, regulation of cell-cell adhesion, nucleoside monophosphate metabolic process, and glycoprotein metabolic process (Figure 3B). The above pathways may therefore participate in regulating the bone miner density.

KEGG pathway analysis revealed that upregulated genes were primarily enriched in pathways associated with the glycine, serine and threonine metabolism, ABC transporters, arginine and proline metabolism, Jak-STAT signaling pathway, RNA degradation, and herpes simplex infection (Figure 3C). In accordance with the enriched GO terms, the up-regulated genes were significantly enriched in inflammation-related pathways. Downregulated genes were mainly associated with adipocytokine signaling pathway, metabolic pathways, oxidative phosphorylation, cytosolic DNA-sensing pathway, and glycerophospholipid metabolism (Figure 3D). The GO and KEGG enrichment analysis of the down-regulated genes suggested that metabolic pathways above may function by maintaining the bone miner density.

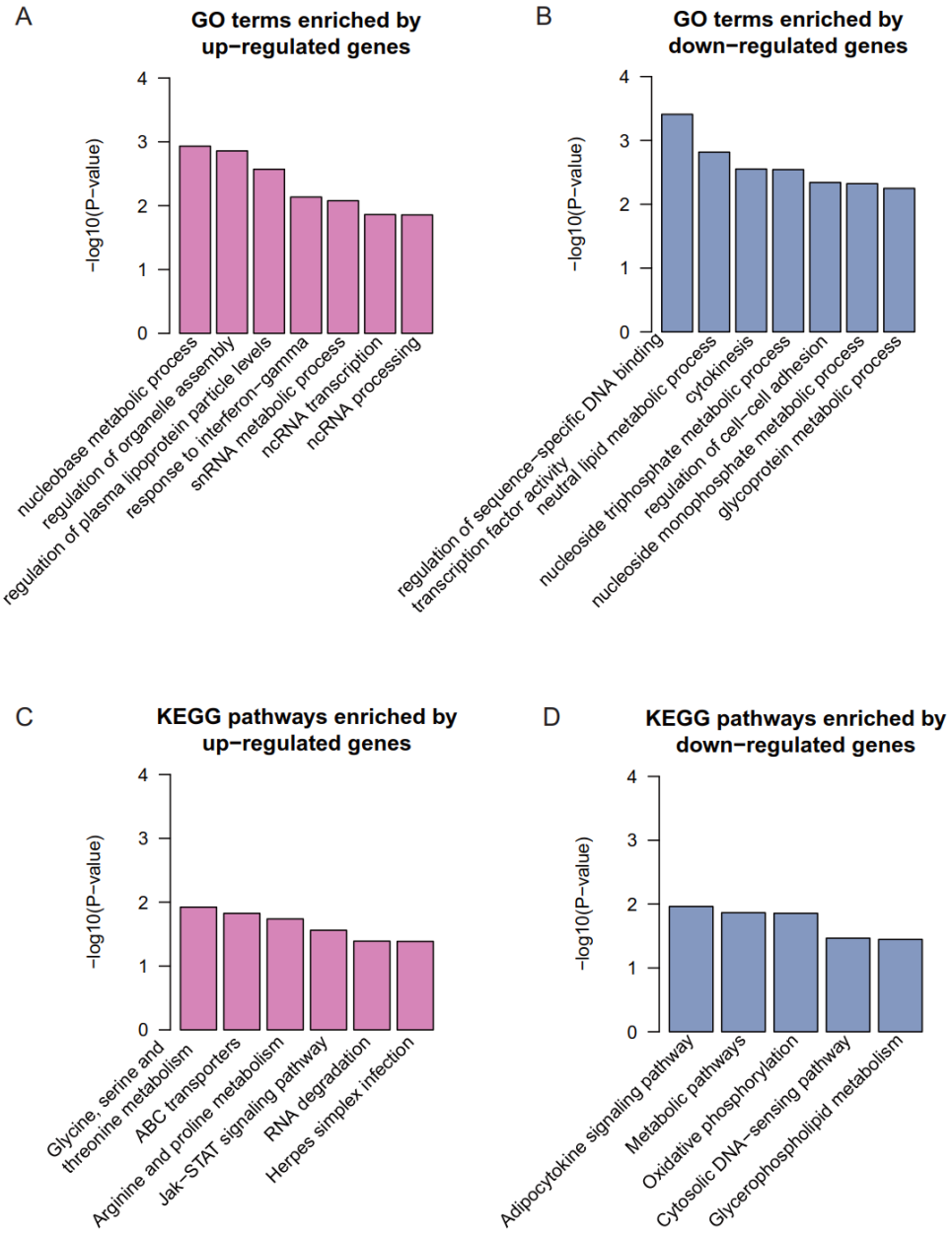

Figure 3. GO and KEGG pathway enrichment analysis for the differentially expressed mRNAs. The enriched GO terms and KEGG pathways for up- and down-regulated genes are presented in (A and B), and (C and D), respectively. The height of each bar represents the -log10-transformed *P*-value. The GO terms and pathway names are listed below the bars.

3.4. PPI network construction for DE-mRNAs

To investigate the interactions between the proteins encoded by the DEGs, we mapped the DEGs to protein-protein interaction network (Figure 4). The PPI network for the upregulated genes contained 38 nodes and 33 edges, and the hub nodes with the higher connectivity degree were SHMT1, MYLIP, MKRN1 and EXOSC8 (connectivity degree = 4, Figure 4A). The PPI network for the downregulated genes contained 198 nodes and 348 edges, and the hub nodes with the higher

connectivity degree were IL8 (connectivity degree = 28), NFKBIA (connectivity degree = 13), HADC5 (connectivity degree = 12) and HDAC4 (connectivity degree = 12) (Figure 4B).

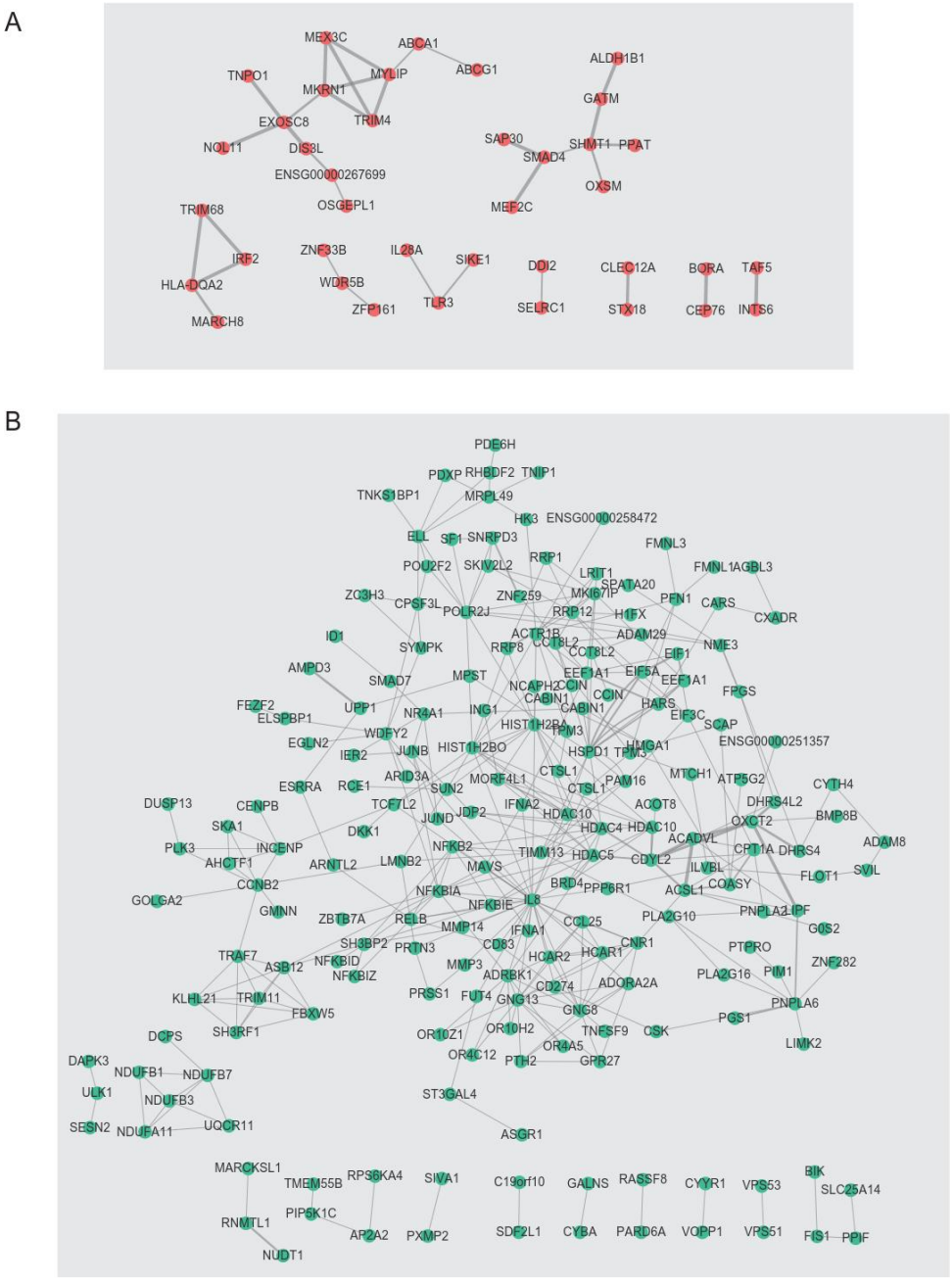

Figure 4. The PPI network of differentially expressed genes. The PPI network for up- and down-regulated genes are presented in (A) and (B), and colored by red and green, respectively.

Furthermore, we also performed a module analysis of the network using MCODE plugin. With degree cut-off $\geqslant$3, four up-regulated proteins, including MEX3C, MKRN1, TRIM4 and MYLIP, were identified as key proteins/genes of a module in the up-regulated PPI network (Figure 5A). The high connectivity and components of a module suggested that MKRN1 and MYLIP may play

important roles in regulating bone miner density. Similarly, the down-regulated proteins, including JDP2, HADC4, HDAC5, CDYL2, ACADVL, ACSL1 and BRD4, were identified as key proteins/genes in the down-regulated PPI network (Figure 5B). Moreover, IL8, CCL25, CNR1, HCAR2, HCAR1, GNG13 and GNG8 were also identified as a module in the down-regulated PPI network (Figure 5C). All these proteins except IL8 participated in G-alpha (i) signaling events, indicating that this pathway may be important for bone mineral homeostasis.

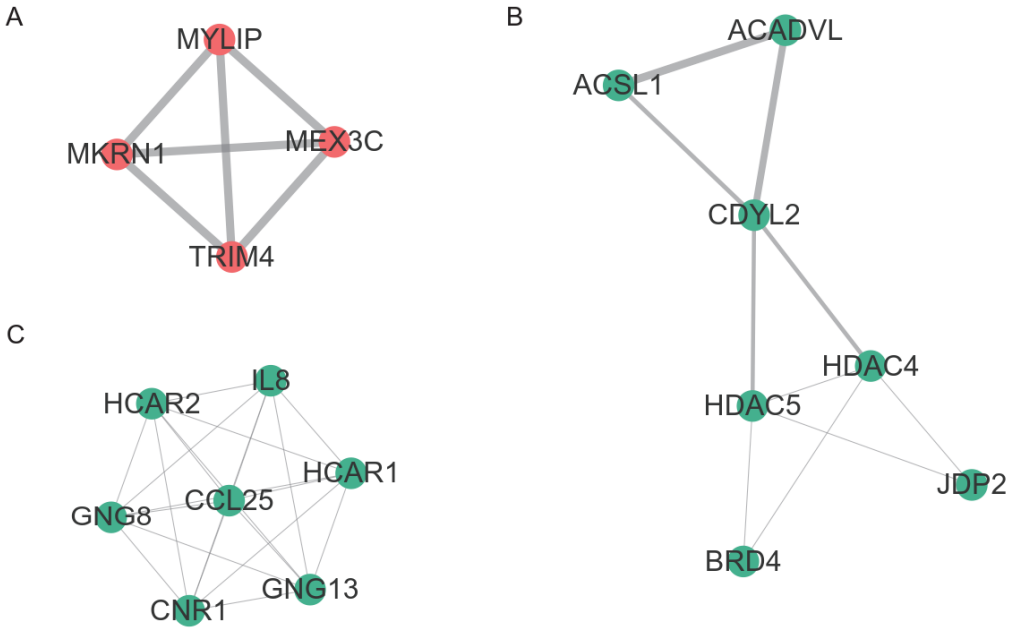

Figure 5. The PPI subnetwork for up- and down-regulated genes by module analysis. The up- and down-regulated genes are colored by red and green.

3.5. Co-expression network analysis of differently expressed mRNAs and lncRNAs in osteoporosis

To predict the potential functional roles of the differentially expressed lncRNAs, the Pearson correlation coefficient for lncRNA-DE-mRNA pairs was first calculated according to their expression value. The co-expressed mRNA-lncRNA pairs with an absolute value of their Pearson correlation coefficient of $\geqslant$0.8 were selected. As presented in Figure 6A, the network included 7 differentially expressed lncRNAs and 70 DE-mRNAs.

To characterize the biological function of the 7 differentially expressed lncRNAs, we performed gene set enrichment analysis on the highly correlated DE-mRNAs. Based to the GO terms by enrichment analysis, we successfully annotated 6 of the 7 DE-lncRNAs ($P < 0.05$, Figure 6B). Specifically, AC009041.1 and SSTR5-AS1 were primarily enriched in DNA conformation change and DNA recombination. Particularly, RP11-498C9.17 was enriched in pathways involved in epigenetic regulation, such as macromolecule deacylation, epigenetic regulation of gene expression, chromatin remodeling, chromatin assembly or disassembly and protein-DNA complex subunit organization. Other lincRNAs may participate in pathways such as cell-cell signaling by Wnt, response to extracellular stimulus, autophagy, and cell cycle checkpoint.

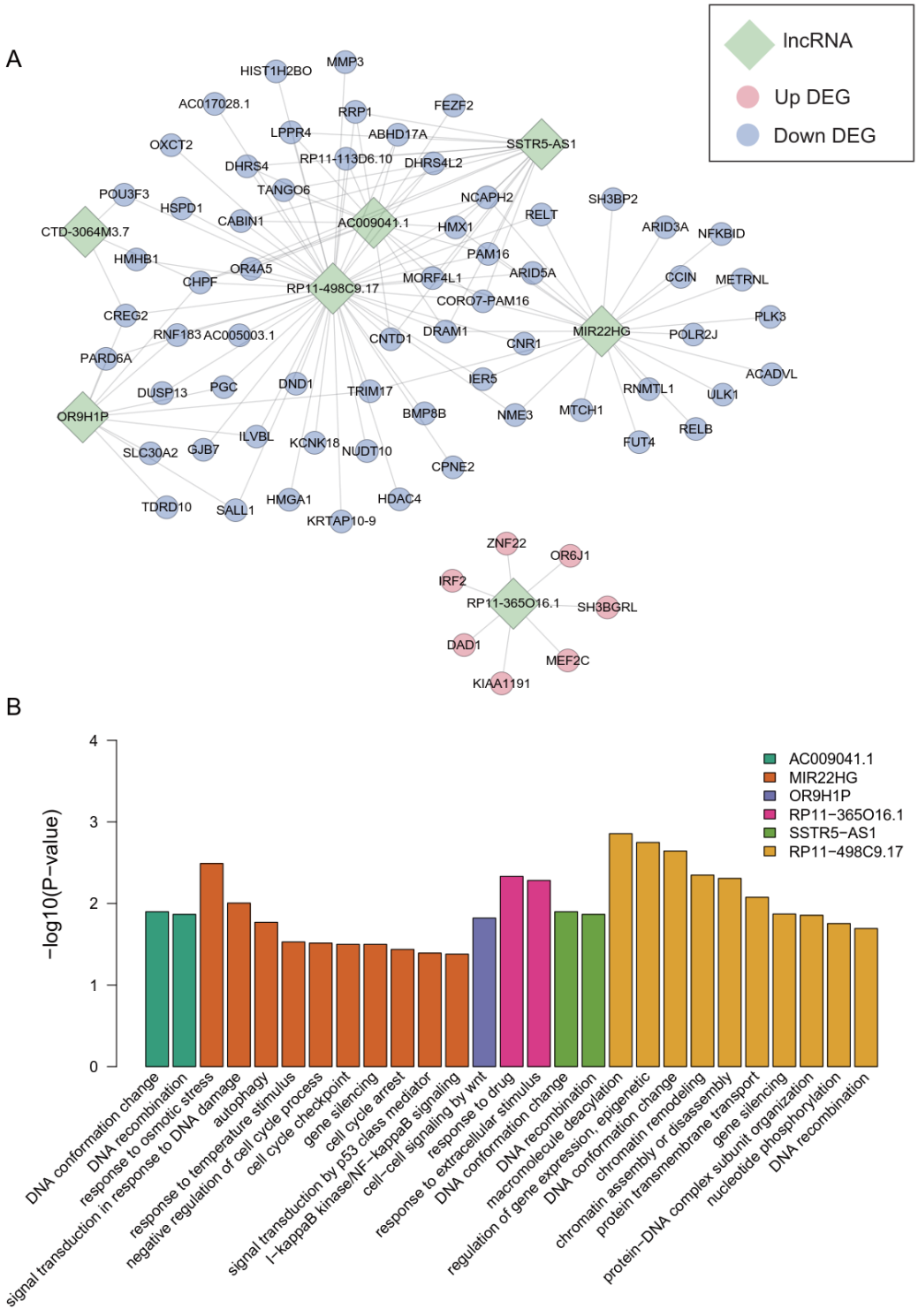

Figure 6. Prediction of biological function of lncRNAs by lncRNA and mRNA co-expression analysis. A. Co-expression network of lncRNAs and mRNAs. The diamonds, red circles and green circles represent the lncRNAs, up-regulated mRNAs, and down-regulated mRNAs. B. The predicted biological functions for lncRNAs. The height of each bar represents the -log10-transformed P-value. Each lncRNA is represented by one specific color. The GO terms are listed below the bars.

4. Discussion

Osteoclastogenesis and bone resorption play a fundamental role in osteoporosis pathogenesis. Better understanding the regulation of osteoclastogenesis is very important for the discovery of therapeutic targets for the treatment of osteoporosis.

In this study, we aimed to analyze the key mRNAs and lncRNAs in osteoporosis. To explore the molecular mechanism of regulating bone miner density, we collected gene expression datasets of peripheral blood monocytes (PBMs) from low or high BMD subjects. To identify the probes on the array corresponding to long non-coding RNA (lncRNA) sequences, we re-annotated all probes using GENCODE gene annotation, and identified a total of 830 long non-coding RNAs.

To investigate the biological differences between samples with low and high BMD, we performed differential expression analysis of the gene expression data from the discovery datasets, and identified a total of 496 differentially expressed genes (DEGs), including 120 up-regulated and 376 down-regulated in low BMD subjects, of which, 24 were long non-coding RNAs differentially expressed between samples with low and high BMD. Subsequently, the differentially expressed mRNAs were subjected to GO and KEGG analyses. The up-regulated mRNAs were significantly enriched in inflammation-related pathways, which was consistent with the conclusion that inflammatory condition could contribute to the differentiation from monocyte to osteoclast by previous study [25]. In contrast, the downregulated genes were mainly associated with adipocytokine signaling pathway, metabolic pathways, oxidative phosphorylation, cytosolic DNA-sensing pathway, and glycerophospholipid metabolism, suggesting that metabolic pathways may function by maintaining the bone miner density.

To investigate the interactions between the proteins encoded by the DEGs, we mapped the DEGs to protein-protein interaction network. We observed that the down-regulated proteins, including JDP2, HADC4, HDAC5, CDYL2, ACADVL, ACSL1 and BRD4, were key components in the down-regulated PPI network (Figure 5B). It is well established that the downregulation of histone deacetylases can promote osteoclastogenesis [26,27], indicating that the downregulation of histone deacetylases and cofactors, such as, HDAC4, HDAC5 and JDP2 may be critical regulators in osteoclastogenesis. Moreover, IL8, CCL25, CNR1, HCAR2, HCAR1, GNG13 and GNG8 were also identified as a module in the down-regulated PPI network (Figure 5C). All these proteins except IL8 participated in G-alpha (i) signaling events, which could inhibit cAMP dependent pathway [28]. Previous study [29] also reported that cAMP-PKA could regulate osteoclast differentiation, indicating that this pathway may be important for bone mineral homeostasis.

To predict the potential functional roles of the differentially expressed lncRNAs, the Pearson correlation coefficient for lncRNA-DE-mRNA pairs was calculated to construct the co-expression network for mRNAs and lncRNAs. Particularly, RP11-498C9.17 was highly correlated with epigenetic regulators, such as HDAC4, MORF4L1, HMGA1 and DND1. As we described above, the downregulation of histone deacetylases can promote osteoclastogenesis, indicating that the lncRNA RP11-498C9.17 may play a key role in bone mineral homeostasis via controlling osteoclastogenesis.

In conclusion, our integrative analysis revealed key mRNAs and lncRNAs, involved in bone mineral homeostasis and osteoclastogenesis. The results not only broaden our insights into lncRNAs in bone mineral homeostasis and osteoclastogenesis, but also improved our understanding of molecular mechanism.

Acknowledgements

This work were financially supported by the Doctoral Fund of Inner Mongolia Normal University under Grant No. 100900091719, the Scientific research projects of the Inner Mongolian higher educational system（NJZY19025）and Provincial Nature Science Research Project of Anhui Colleges (KJ2018A0331). The funders had no role in study design, data collection and analysis, decision to publish, or preparation of the manuscript.

Conflict of interest

The authors declare that they have no competing interests.

Availability of data and materials

The analyzed data sets generated during the study are available from GEO database.

Authors' contributions

Ruidong Zhang, Li Li and Xueqing Wang performed the experiments and data analysis. Xiaoting Liu and Rui Guo collected rawdata. Ruidong Zhang wrote the manuscript. Li Li and Xueqing Wang revised the manuscript. All authors read and approved the final manuscript.

Ethical approval and consent to participate

Not applicable.

References

1. O. Johnell and J. A. Kanis, An estimate of the worldwide prevalence and disability associated with osteoporotic fractures, *Osteoporosis Int.*, **17** (2006), 1726–1733.
2. B. Abrahamsen, P. Vestergaard, B. Rud, et al., Ten-year absolute risk of osteoporotic fractures according to BMD T score at menopause: The danish osteoporosis prevention study, *J. Bone Miner Res.*, **21** (2006), 796–800.
3. J. A. Kanis, H. Johansson, A. Oden, et al., A family history of fracture and fracture risk: A meta-analysis, *Bone*, **35** (2004), 1029–1037.
4. J. A. Kanis, O. Johnell, C. De Laet, et al., A meta-analysis of previous fracture and subsequent fracture risk, *Bone*, **35** (2004), 375–382.
5. J. A. Kanis, H. Johansson, A. Oden, et al., A meta-analysis of prior corticosteroid use and fracture risk, *J. Bone Miner Res.*, **19** (2004), 893–899.
6. J. A. Kanis, H. Johansson, O. Johnell, et al., Alcohol intake as a risk factor for fracture, *Osteoporosis Int.*, **16** (2005), 737–742.
7. J. A. Kanis, O. Johnell, A. Oden, et al., Smoking and fracture risk: A meta-analysis, *Osteoporosis Int.*, **16** (2005), 155–162.
8. R. E. Cole, Improving clinical decisions for women at risk of osteoporosis: dual-femur bone

mineral density testing, *J. Ost. Ass.*, **108** (2008), 289–295.
9. K. Ikedaand S. Takeshita, Factors and mechanisms involved in the coupling from bone resorption to formation: how osteoclasts talk to osteoblasts, *J. Bone Miner. Metab.*, **21** (2014), 163–167.
10. T. Sudaand N. Takahashi, Origin of osteoclasts and the role of osteoblasts in osteoclast differentiation, *J. Orthop. Sci.*, **65** (1991), 261–270.
11. E. Terposand E. Voskaridou, Interactions between osteoclasts, osteoblasts and immune cells: implications for the pathogenesis of bone loss in thalassemia, *Pediatr. Endocr. Rev. P.*, **6 Suppl 1** (2008), 94–106.
12. X. F. Chen, D. L. Zhu, M. Yang, et al., An Osteoporosis Risk SNP at 1p36.12 Acts as an Allele-Specific Enhancer to Modulate LINC00339 Expression via Long-Range Loop Formation, *Am. J. Hum. Genet.*, **102** (2018), 776–793.
13. T. Uranoand S. Inoue, Genetics of osteoporosis, *Biochem. Bioph. Res. Co.*, **452** (2014), 287–293.
14. A. D. Real, L. Rianchozarrabeitia, L. Lopezdelgado, et al., Epigenetics of skeletal diseases, *Curr. Osteoporos. Rep.*, **16** (2018), 246–255.
15. D. Bellavia, A. De Luca, V. Carina, et al., Deregulated miRNAs in bone health: Epigenetic roles in osteoporosis, *Bone*, **122** (2019), 52–75.
16. S. Reppe, T. G. Lien, Y. H. Hsu, et al., Distinct DNA methylation profiles in bone and blood of osteoporotic and healthy postmenopausal women, *Epigenetics-US*, **12** (2017), 674–687.
17. S. D. Jiang, L. S. Jiangand L. Y. Dai, Effects of spinal cord injury on osteoblastogenesis, osteoclastogenesis and gene expression profiling in osteoblasts in young rats, *Osteoporosis Int.*, **18** (2007), 339–349.
18. Y. Bae, T. Yang, H. C. Zeng, et al., miRNA-34c regulates Notch signaling during bone development, *Hum. Mol. Genet.*, **21** (2012), 2991–3000.
19. X. Ji, X. Chenand X. Yu, MicroRNAs in Osteoclastogenesis and Function: Potential Therapeutic Targets for Osteoporosis, *Int. J. Mol. Sci.*, **17** (2016), 349.
20. Y. Xiu, H. Xu, C. Zhao, et al., Chloroquine reduces osteoclastogenesis in murine osteoporosis by preventing TRAF3 degradation, *J. Clin. Invest.*, **124** (2014), 297–310.
21. P. D'Amelio, A. Grimaldi, S. Di Bella, et al., Estrogen deficiency increases osteoclastogenesis up-regulating T cells activity: a key mechanism in osteoporosis, *Bone*, **43** (2008), 92–100.
22. Y. Z. Liu, Y. Zhou, L. Zhang, et al., Attenuated monocyte apoptosis, a new mechanism for osteoporosis suggested by a transcriptome-wide expression study of monocytes, *PloS one*, **10** (2015), e0116792.
23. J. Wang, S. Vasaikar, Z. Shi, et al., WebGestalt 2017: a more comprehensive, powerful, flexible and interactive gene set enrichment analysis toolkit, *Nucleic Acids Res.*,**45** (2017), W130–W137.
24. D. Szklarczyk, J. H. Morris, H. Cook, et al., The STRING database in 2017: quality-controlled protein-protein association networks, made broadly accessible, *Nucleic Acids Res.*, **45** (2017), D362–D368.
25. K. Yokota, Inflammation and osteoclasts, *J. Clin. Immunol.*, **40** (2017), 367–376.
26. E. W. Bradley, L. R. Carpio, A. J. van Wijnen, et al., Histone Deacetylases in Bone Development and Skeletal Disorders, *Physiol. Rev.*, **95** (2015), 1359–1381.
27. N. C. Blixt, B. K. Faulkner, K. Astleford, et al., Class II and IV HDACs function as inhibitors of osteoclast differentiation, *PloS one*, **12** (2017), e0185441.
28. C. W. Dessauer, M. Chen-Goodspeed and J. Chen, Mechanism of Galpha i-mediated inhibition of type V adenylyl cyclase, *J. Biol. Chem.*, **277** (2002), 28823–28829.

29. G. Ramaswamy, H. Kim, D. Zhang, et al., Gsalpha controls cortical bone quality by regulating osteoclast differentiation via cAMP/PKA and β-Catenin pathways, *Sci. Rep-UK*, **7** (2017), 45140.

AIMS Press